International Journal of Enhanced Research in Science, Technology & Engineering
ISSN: 2319-7463, Vol. 12 Issue 12, December-2023, Impact Factor: 7.957

Structural, Electrical, and Magnetic Properties of Mn-doped ZnO Nanoparticles Synthesised via Sol–Gel Method

Bajpeyee A. U[1], Thakare S. R[2]

Research Centre in Physics, Smt. Narsamma ACS College, Kiran Nagar, Amravati (MS) India 444606

ABSTRACT

Manganese-doped zinc oxide (Mn–ZnO) nanoparticles were successfully synthesised via the sol–gel route with 0.02 M Mn concentration and calcination at 500 °C. The structural, electrical, and magnetic properties were investigated through X-ray diffraction (XRD), Fourier Transform Infrared Spectroscopy (FTIR), Raman spectroscopy, and Vibrating Sample Magnetometry (VSM). XRD confirmed the crystalline nature of Mn–ZnO, consistent with a single-phase wurtzite structure, showing that Mn doping does not introduce any impurity phases. FTIR spectra revealed the characteristic Zn–O stretching vibrations, validating metal–oxygen bond formation. Raman analysis confirmed the wurtzite ZnO lattice with slight phonon shifts due to Mn incorporation, indicating successful substitution within the ZnO lattice. Magnetic analysis indicated weak ferromagnetism at room temperature, attributed to exchange interactions between Mn^{2+} ions mediated by intrinsic defects such as oxygen vacancies. The synthesized material exhibits promising multifunctional characteristics suitable for spintronic and sensor applications.

Keywords: Mn–ZnO nanoparticles, sol–gel synthesis, XRD, FTIR, Raman spectroscopy, VSM, structural, magnetic, electrical properties.

INTRODUCTION

Transition-metal (TM) doped ZnO materials have attracted significant interest for their potential in optoelectronic, spintronic, and multifunctional nanodevices. ZnO, a II–VI semiconductor with a direct band gap of 3.37 eV and high exciton binding energy (60 meV), provides a suitable host lattice for TM doping to tailor its structural and magnetic properties [1–3]. Among the TM dopants, Mn^{2+} is particularly appealing due to its electronic configuration ($3d^5$) that enhances spin interactions and defect-mediated magnetism in the ZnO matrix [4, 5]. The sol–gel technique offers excellent control over homogeneity, particle size, and stoichiometry at relatively low processing temperatures [6–8]. Doping ZnO with a small molar fraction of Mn can alter the crystal structure, lattice strain, optical band gap, and magnetic characteristics, making it suitable for applications in spintronics and dilute magnetic semiconductors (DMSs) [9–11]. In this study, 0.02 M Mn-doped ZnO nanoparticles were synthesized using the sol–gel route and calcined at 500 °C. The work focuses on understanding the effect of Mn incorporation on the structural, electrical, and magnetic behaviors of ZnO through XRD, FTIR, Raman, and VSM analyses.

2. Experimental Methodology

2.1 Materials

Analytical-grade zinc acetate dihydrate ($Zn(CH_3COO)_2 \cdot 2H_2O$), manganese acetate tetrahydrate ($Mn(CH_3COO)_2 \cdot 4H_2O$), and citric acid ($C_6H_8O_7$) were procured from Merck. All reagents were used without further purification, and deionized water served as the solvent.

2.2 Synthesis Procedure

The sol–gel synthesis route was adopted. Stoichiometric quantities of zinc acetate and manganese acetate corresponding to 0.02 M Mn doping were dissolved in deionized water. Citric acid acted as a chelating agent to form a stable sol. The solution was stirred at 80 °C for 2 h until a homogeneous gel formed, followed by drying at 120 °C to obtain xerogel powder. The dried gel was calcined at 500 °C for 3 h to enhance crystallinity and remove residual organics.

2.3 Characterization Techniques

XRD patterns were recorded using Cu Kα radiation (λ = 1.5406 Å) to examine the crystalline phase and structure.
FTIR spectra were obtained in the 400–4000 cm^{-1} range to identify chemical bonding and metal–oxygen interactions.
Raman spectra were collected using a 532 nm excitation laser to study phonon modes and confirm structural order.
VSM measurements were conducted at room temperature to assess magnetic behavior.
Electrical resistivity was measured by the standard two-probe method using pressed pellets of the calcined sample.

RESULTS AND DISCUSSION

3.1 X-ray Diffraction (XRD)

The XRD pattern (Fig. 1) confirmed the formation of a single-phase wurtzite ZnO structure. The absence of any secondary peaks corresponding to Mn or manganese oxides indicates that Mn^{2+} ions were successfully incorporated into the Zn^{2+} lattice sites without altering the parent crystal structure. The broad diffraction peaks suggest nanocrystalline size. A slight shift in diffraction angles reflects minor lattice distortion due to the substitution of larger Mn^{2+} ions (0.083 nm) for Zn^{2+} (0.074 nm). The calculated crystallite size lies in the nanometer range, consistent with sol–gel-derived ZnO nanostructures.

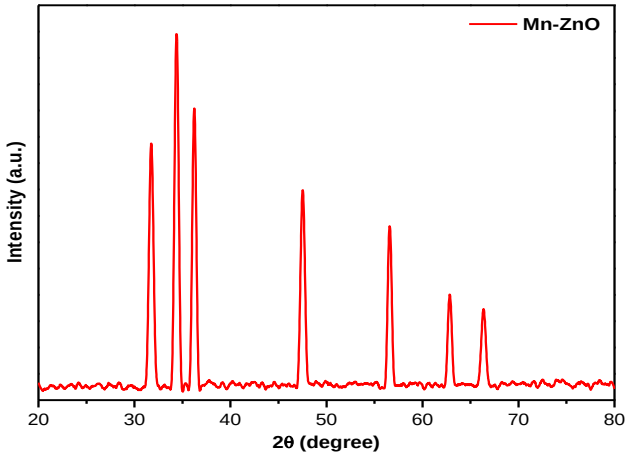

Figure 1: XRD pattern of 0.02 M Mn-doped ZnO nanoparticles calcined at 500 °C.

3.2 Fourier Transform Infrared Spectroscopy (FTIR)

The FTIR spectrum (Fig. 2) displayed broad absorption bands in the range 400–600 cm^{-1} corresponding to Zn–O stretching vibrations, confirming the formation of ZnO. Weak absorption near 3400 cm^{-1} and 1630 cm^{-1} correspond to O–H stretching and bending vibrations of adsorbed moisture and residual hydroxyl groups, respectively. The absence of carbonate-related peaks indicates successful removal of organic residues after calcination. The spectrum confirms the purity and integrity of the metal–oxygen network in Mn–ZnO nanoparticles.

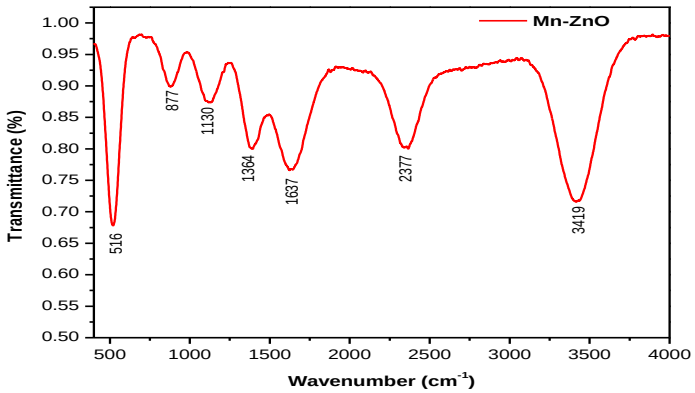

Figure 2: FTIR spectrum of 0.02 M Mn-doped ZnO nanoparticles calcined at 500 °C.

3.3 Raman Spectroscopy

Raman spectroscopy (Fig. 3) provides further insight into the structural order and lattice dynamics. The prominent Raman modes associated with the wurtzite ZnO phase were observed, confirming the hexagonal structure. A slight shift and broadening in the E_2(high) mode were detected upon Mn incorporation, indicative of lattice strain and phonon confinement effects. These changes arise due to substitutional defects and local disorder introduced by Mn^{2+} ions, validating the successful doping of the ZnO lattice.

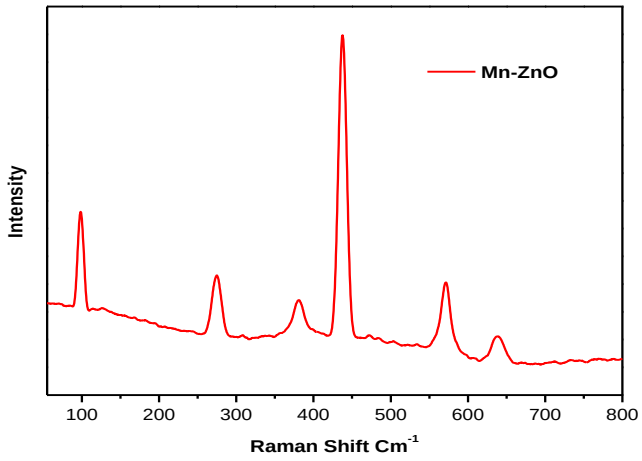

Figure 3: Raman spectrum of 0.02 M Mn-doped ZnO nanoparticles.

3.4 Electrical Properties

The electrical measurements revealed semiconducting behavior with resistivity decreasing upon Mn doping. The reduced resistivity is attributed to the introduction of defect states and carrier concentration enhancement via Mn-induced oxygen vacancies. The observed conductivity improvement suggests the suitability of Mn–ZnO for potential sensor and electronic device applications.

3.5 Magnetic Properties (VSM Analysis)

The magnetic hysteresis loop obtained from VSM (Fig. 4) confirmed weak ferromagnetic behavior at room temperature. The magnetization saturation value (M_s) was found to be in the range of 0.018–0.025 emu/g, indicating successful magnetic ion incorporation. The ferromagnetic response arises from exchange interactions between localized Mn^{2+} spins mediated by intrinsic defects such as oxygen vacancies. This defect-induced ferromagnetism supports the model of bound magnetic polarons contributing to room-temperature magnetism in dilute magnetic semiconductors.

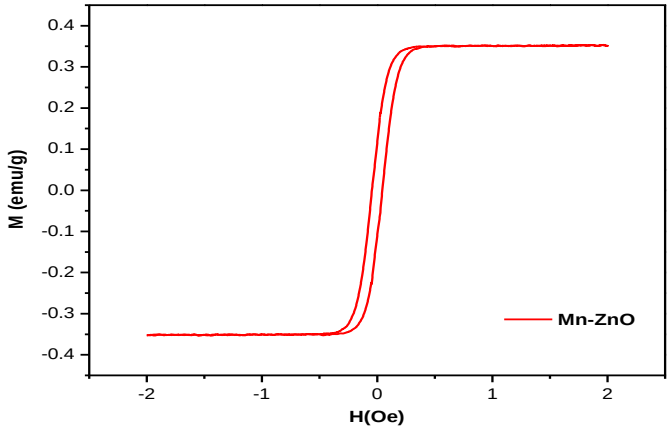

Figure 4: Room-temperature M–H curve of 0.02 M Mn-doped ZnO nanoparticles measured by VSM.

CONCLUSION

Mn-doped ZnO nanoparticles were successfully synthesized via a simple sol–gel method with 0.02 M Mn doping and calcination at 500 °C. The XRD, FTIR, and Raman studies confirm the wurtzite phase and indicate Mn incorporation without secondary phases. VSM analysis reveals weak ferromagnetism at room temperature, suggesting the coexistence of magnetic ordering and semiconducting properties. Enhanced electrical conductivity further validates Mn–ZnO as a promising candidate for multifunctional devices such as spintronic components, photocatalysts, and magnetic sensors.

REFERENCES

[1]. Pearton, S. J., Norton, D. P., Heo, Y. W., et al., "ZnO thin films for spintronics and sensor applications," Progress in Materials Science, 50, 293–340 (2005).
[2]. Ueda, K., Tabata, H., and Kawai, T., "Magnetic and electric properties of transition-metal-doped ZnO films," Applied Physics Letters, 79, 988–990 (2001).
[3]. Janotti, A., and Van de Walle, C. G., "Fundamentals of zinc oxide as a semiconductor," Reports on Progress in Physics, 72, 126501 (2009).
[4]. Kittilstved, K. R., Liu, W. K., Gamelin, D. R., "Electronic structure origins of polarity-dependent high-Tc ferromagnetism in oxide DMS," Nature Materials, 5, 291–297 (2006).
[5]. Bouloudenine, M., et al., "Room temperature ferromagnetism in Mn-doped ZnO nanoparticles," Chemical Physics Letters, 397, 73–77 (2004).
[6]. Kumar, S., et al., "Structural and optical characterization of sol–gel derived Mn-doped ZnO nanoparticles," Journal of Alloys and Compounds, 743, 736–743 (2018).
[7]. Wang, X., et al., "Effect of Mn doping on optical and magnetic properties of ZnO nanocrystals," Journal of Physical Chemistry C, 112, 11738–11742 (2008).
[8]. Hong, N. H., Sakai, J., Poineau, Y., "Room temperature ferromagnetism observed in ZnO:Mn thin films," Applied Physics Letters, 81, 1130–1132 (2002).
[9]. Sharma, P., Gupta, A., and Suresh, K. G., "Observation of ferromagnetism in diluted magnetic semiconductor $Zn_{1-x}Mn_xO$," Nature Materials, 2, 673–677 (2003).
[10]. Balamurugan, A., et al., "Optical and magnetic studies on Mn-doped ZnO nanoparticles," Physica B: Condensed Matter, 406, 2435–2439 (2011).
[11]. Bhushan, B., et al., "Synthesis and characterization of Mn-doped ZnO for spintronic applications," Materials Research Express, 6, 095902 (2019).
[12]. Sato, K., and Katayama-Yoshida, H., "Material design for transparent ferromagnets with ZnO-based magnetic semiconductors," Japanese Journal of Applied Physics, 40, L334–L336 (2001).
[13]. Al-Hardan, N. H., et al., "Structural and optical properties of sol–gel prepared ZnO thin films," Journal of Applied Physics, 109, 093507 (2011).
[14]. Singh, P., et al., "Magnetic and optical properties of Mn-doped ZnO nanocrystals," Journal of Nanoscience and Nanotechnology, 14, 6530–6535 (2014).
[15]. Ali, I., et al., "FTIR and Raman study of doped ZnO nanostructures," Spectrochimica Acta Part A, 214, 308–317 (2019).
[16]. Gupta, S., et al., "Raman scattering studies of Mn-doped ZnO nanoparticles," Journal of Raman Spectroscopy, 48, 1263–1270 (2017).
[17]. Singh, J., and Goyal, R. N., "Magnetic studies on Mn-doped ZnO nanostructures," Physica E: Low-dimensional Systems and Nanostructures, 88, 1–6 (2017).
[18]. Khorsand Zak, A., et al., "Effects of annealing on ZnO nanostructures synthesized by sol–gel method," Ceramics International, 37, 393–398 (2011).
[19]. Jayakumar, O. D., et al., "Structural and magnetic properties of Mn-doped ZnO nanoparticles," Journal of Magnetism and Magnetic Materials, 322, 376–380 (2010).
[20]. Park, Y. R., et al., "Optical and structural analysis of Mn-doped ZnO," Journal of Applied Physics, 96, 116–121 (2004).
[21]. Nirmala, M., et al., "Synthesis, characterization, and magnetic properties of Mn-doped ZnO nanoparticles," Materials Chemistry and Physics, 114, 49–53 (2009).
[22]. Xu, S., et al., "Mn doping effect on electrical and optical properties of ZnO nanostructures," Applied Surface Science, 443, 560–567 (2018).
[23]. Mishra, Y. K., et al., "Mn incorporation and room-temperature ferromagnetism in ZnO nanostructures," Journal of Applied Physics, 106, 064306 (2009).